TID-4500, UC-34
Physics

LAWRENCE LIVERMORE LABORATORY
University of California/Livermore, California/94550

UCRL-51353

THE ROLE OF Li_2O ON THERMOLUMINESCENCE IN 7LiF

Arthur J. Toy
(Ph.D. Thesis)

MS. date: March 28, 1973

Contents

List of Figure Captions

List of Tables

THE ROLE OF Li_2O ON THERMOLUMINESCENCE IN ^7LiF

Abstract

Li_2O was added to pure ^7LiF, and single crystals with varying amounts of oxygen were grown. The thermoluminescent response of these crystals to ionizing radiation indicates that the added oxygen functions as a luminescence center.

Introduction

This investigation was made to study the effect of Li_2O on the thermoluminescence (TL) of LiF. Thermoluminescence may be defined by the following sequence of events:

1. Energy is absorbed by a crystalline solid.
2. Some of this energy is stored in metastable energy states, called "traps."
3. Upon heating, some of this stored energy is released as visible or ultraviolet light.

Many materials are thermoluminescent, and many investigators[1-6] have used TL to infer the ionizing radiation dose (energy absorbed per unit mass) to these materials.

One thermoluminescent material now being widely used for personnel dosimetry is lithium fluoride (LiF). LiF has several advantages which lead to its acceptance:[1]

1. It has an effective atomic number approximately equal to that of soft tissue.

2. Its sensitivity, or TL output per unit dose, is (a) independent of dose rate for rates less than 10^{11} rad/sec;[7] (b) independent of dose for doses less than 1000 rad; (c) sufficient to be able to detect doses of 1 mrad; and (d) sensibly independent of storage time after exposure (less than 5% signal loss per year at room temperature).

The LiF that is being used for personnel dosimetry is not "pure" since it has been found that the addition of selected impurities improves the sensitivity.[1]

The Harshaw Chemical Company, a producer of LiF thermoluminescent dosimeters (TLD) has a patent* for these TLD's covering the addition of some specific elements to make a more sensitive TLD.

The LiF TLD phosphors produced by the Harshaw Chemical Company contain ~100-200 ppm Mg and 10-20 ppm Ti.[8] These dosimeters, called TLD-100 (natural isotopic composition of lithium), TLD-600 (~95% ^6Li), or TLD-700

*Phosphors (to the Harshaw Chemical Co.), British Patent, 1,059,518 (1967). Reference to a company or product name does not imply approval or recommendation of the product by the University of California or the U.S. Atomic Energy Commission to the exclusion of others that may be suitable.

(~100% ^{7}Li)[1] are widely used for dosimetric purposes. Considerable effort has been expended to determine the details of the TL mechanism of Harshaw TLD's and LiF doped with these same impurities (termed LiF:Mg or LiF:Mg, Ti).[9-16]

Figure 1 is the "glow curve" that results when LiF:Mg is heated following irradiation. The glow curve is conventionally resolved into the individual components, as shown, and each component is thought to result from a single type of metastable trap.[17]

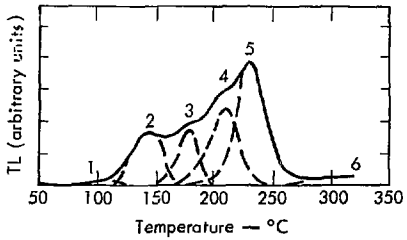

Fig. 1. Glow curve of LiF:Mg exposure—800R, heating rate -- 3°C/sec.

Figure 2 is an optical absorption spectrum of irradiated LiF:Mg. The dashed curves show the resolution into single bands, which are associated with various crystal defects as follows[17]:

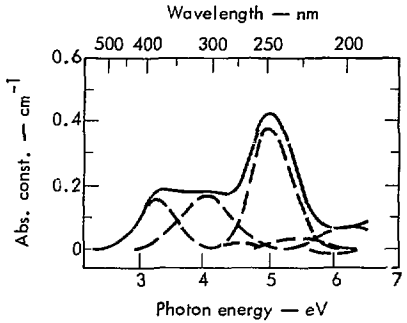

Fig. 2. Optical absorption spectrum of LiF:Mg.

- 380- and 310-nm bands—related to Mg impurity.
- 250 nm—F band (an electron in an anion lattice position) produced by the irradiation.
- 200 nm—Impurity band (Ti causes an absorption band here).[18]
- 22[illegible] nm—Z_3 band (a Z_3 center is an F center with one of the nearest Li^+ ions replaced by an Mg^{++} ion).[19]

The glow curve shape can be modified (by annealing) to emphasize peaks 4 and 5.[10] These peaks occur at a temperature enough above ambient temperature to minimize fading. Since most dosimetry is done using peaks 4 and 5, most of the work on the mechanism of TL in LiF has been directed toward that part of the TL which involves those peaks.

The currently accepted mechanism for TL in LiF:Mg, Ti is as follows[16]:

- Ionizing radiation produces a free electron which is trapped in a Mg-related, trap and is probably Mg^{++} associated with a nearby cation vacancy. The 310-nm absorption band is correlated with peaks 4 and 5 of the glow curve.
- Subsequent heating releases the trapped electron to the conduction band.
- The electron encounters a V_3 center (an F_2 molecule) and annihilates one of the holes of the V_3 center, producing a V_k center.
- Since the V_k center is unstable above 160°K, the second hole is released.

• This mobile hole can recombine at a luminescence center (involving Ti) to emit a photon.

Several investigators[9,20,21] have wondered what role oxygen might have in the TL process in LiF. It has been shown[22] that OH^- inhibits TL, probably by creating competitive electron trapping sites which do not empty during the normal TL heating cycle.

Other forms of oxygen are possible in alkali halides. It has been shown[23] that O_2^- is a luminescence center in other alkali halides. $O^=$ should fit well into the LiF crystal since its ionic radius is similar to that of F^- (0.132 versus 0.133 nm, respectively).[24] The solubility of Li_2O in LiF is limited, however,[25] by structure modification considerations, i.e., the crystal structure of Li_2O changes when it is inserted into the LiF lattice.

Since the starting material for some LiF is LiOH[26] and since LiOH is converted to Li_2O at temperatures greater than 300°C,[27] an attempt was made to discover what effect Li_2O had on the TL of LiF. The possibility that the direct applicability of results would be lost was considered. However, it was decided to restrict the study to a Li_2O, pure LiF system, rather than Li_2O, LiF:Mg, Ti. This was done to limit the possibility that effects due to Li_2O which were small might be missed in the highly thermoluminescent LiF:Mg, Ti.

It was decided to attempt to grow several crystals of LiF with various amounts of Li_2O added to the starting material, analyze the oxygen content of these crystals, and see if correlations existed between oxygen content, optical absorption, and TL.

Materials and Methods

CRYSTAL GROWING

To study the effect of Li_2O on the TL of LiF, single crystals of ^{7}LiF were grown with Li_2O added to the starting material. The starting material for the various crystals was prepared as follows:

Pure ^{7}LiF from the Oak Ridge National Laboratory (ORNL) was used. This LiF was prepared by methods reported elsewhere.[26,28,29] These methods result in total cationic impurities of approximately 30 parts per billion and very low oxygen ($O^=$ and OH^-) content.[29] The fact that the LiF used was ^{7}LiF is not significant in this report; it was used because a supply existed.

After production at ORNL, the ^{7}LiF was flooded with dry helium and sealed in a polyethylene screw-topped vial. The vial was then sealed in a glass vial with dry helium and "vac-sorb" (a dessicant).

The Li_2O was purchased from Research Organic /Inorganic Chemical Corporation in a wax-sealed glass jar. The Li_2O was 99% pure.[30]

All operations with these chemicals, as well as many of the operations on the single crystals, were conducted in a glove box which could either be evacuated (to $<10^{-3}$ Torr) or backfilled with "UHP" (>99.999% pure) helium. A pass-in port was affixed which allowed the introduction

and withdrawal of materials from the glove box without contaminating the glove box atmosphere.

The furnace used for growing crystals is shown schematically in Fig. 3. The crucible was made of high-purity nickel, and was connected to a vacuum system and a UHP helium supply. The two heating elements were individually controllable. The furnace was driven vertically over the crucible.

The rate was controlled by a speed-reducing gear box. The rate of travel of the furnace for all crystal growing operations was 3.8 mm/hr.

To check the temperature gradient, a chromel-alumel thermocouple was inserted through the bottom of the furnace along the axis. The output of the thermocouple was then measured with a Leeds and Northrup Model 8691 millivolt potentiometer. The heating element controllers were adjusted to give a temperature gradient of 10°C/cm at 842°C (the melting point of LiF).

A ball valve was attached to the crucible so that the atmosphere inside the crucible could be controlled.

Before growing any crystals in the crucible, it was cleaned as follows:

1. The interior was "grit-blasted" with 240-mesh SiC.

2. The tip was inspected with a borescope to insure freedom from scratches, pits, and foreign material.

3. The crucible was rinsed with 2*N* HCl, distilled H_2O, acetone and methanol, in that order.

4. The empty crucible was placed in the furnace, evacuated, and then heated to 900°C for 1 hr.

5. After cooling, the ball valve was closed, the crucible was removed from the furnace and placed in the glove box.

After this initial cleaning, the crystals for this investigation were grown in succession. Since each crystal was removed from the crucible without difficulty the crucible was not recleaned, but was stored in the glove box except when it was being used to grow crystals.

To prepare the starting material, load the crucible and grow the crystal, the following procedure was used (steps 1

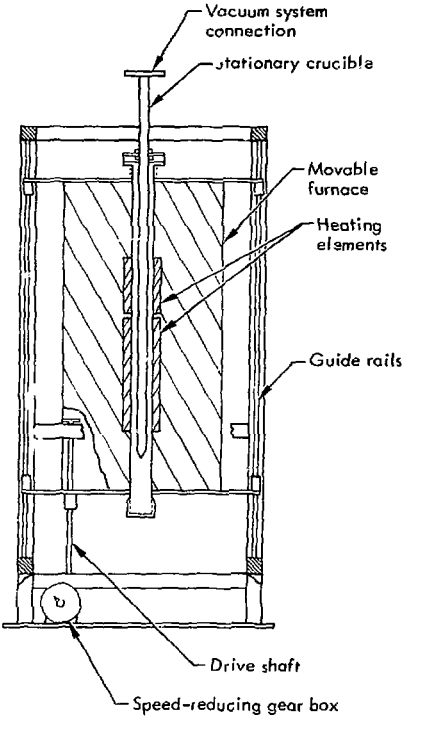

Fig. 3. Furnace for growing single crystals.

through 3 were done in the glove box under an HE atmosphere):

1. 1.2 g of ORNL ^{7}LiF was crushed to <80 mesh. Approximately 6 mg of Li_2O was added and mixed with the LiF. This mixture was used to dope some of the crystals.

2. Pure ORNL ^{7}LiF was crushed to <3 mm. Weighed batches of this material were used to grow the various crystals (see Table 1).

3. The starting material was poured into the crucible, the ball valve was closed and the crucible was removed from the glove box.

4. The crucible was placed in the furnace and the line to the ball valve was evacuated.

5. The ball valve was opened and the entire system was then evacuated, backfilled with UHP He, and evacuated again.

6. The heaters were brought to 600°C and held there for at least 1 hr at which point the crucible was back-filled with UHP He to a pressure of ~0.5/psig.

7. The heaters were brought to crystal-growing temperature and the furnace drive motor was started.

8. When the furnace had reached the top of its travel and the crystal had been grown, the temperature in the furnace was slowly reduced by mechanically driving the controllers downward.

9. After the mechanical rundown of the controllers (at least 16 hr elapsed time), the power to the furnace was turned off and the furnace was allowed to cool to room temperature (at least 4 hr).

10. The valve was closed, the crucible was removed from the furnace and returned to the glove box.

Note that at no time were the starting materials or the crystal exposed to air. This was to prevent the reaction

$$Li_2O + H_2O \rightarrow 2LiOH$$

which has an equilibrium constant, K_{eq}, of 58 at 25°C.[24] The back reaction

$$2LiOH \rightarrow Li_2O + H_2O$$

occurs at "red" heat.[27] Therefore, heating to 600°C for 1 hr under vacuum should serve to convert the LiOH present to Li_2O and remove the water vapor.

Table 1. Composition of starting material for crystal growth.

Crystal designation	ORNL LiF (g)	LiF/Li_2O^{mix} (g)	Li_2O (g)	Added O as ppm (wt/wt)
AJ-3	10.1	0	0	0
AJ-4	10.7	0	0.03	1500
AJ-5	9.65	0.4	—	200
AJ-6	9.9	0.1	—	50

CHEMICAL ANALYSIS

Analysis of the oxygen content of the crystals was done by comparison assay. The amount of oxygen present in selected portions of the crystals AJ-3 through AJ-6 was compared with the amount of oxygen present in standards containing known amounts of ORNL ^{7}LiF and Li_2O.

The samples were prepared for analysis as follows (all operations were done in the glove box, under a UHP He atmosphere):

1. Quantities of ORNL ^{7}LiF and Li_2O were accurately weighed using a Cahn Model 1500 electrobalance.

2. These chemicals were mixed and ground for 5 min in a stainless steel mixing-grinding vessel, in a dental amalgamator. This was enough time to reduce the material to <400-mesh particle size.

3. Successive dilutions were prepared by mixing weighed fractions of a LiF-Li_2O mix with pure ^7LiF.

4. A standard "zero" was prepared by grinding up pure ^7LiF as above.

5. Samples were taken from each of the crystals and ground as above.

6. Each sample or standard was placed in a polyethylene screw top bottle. These bottles were then sealed in a glass jar with "Drierite" to trap any moisture which might be present.

Table 2 gives sample identification and oxygen concentrations for the standards. The amount initially present was determined as in the Results section under Chemical Analysis.

The sealed samples were then delivered to an analytical chemist who performed the analysis using the following reactions:

$$Li_2O + CO_2 \xrightarrow{H_2O} Li_2CO_3$$

$$\frac{3}{2}\,Li_2CO_3 + H_3PO_4 \rightarrow Li_3PO_4 + \frac{3}{2}\,H_2O + \frac{3}{2}\,CO_2.$$

OPTICAL ABSORPTION

Since the reaction

$$2LiOH + CO_2 \rightarrow Li_2CO_3 + H_2O$$

will occur if LiOH is present,[31] the infrared transmissions of cleaved portions of crystals AJ-6 and AJ-4 were measured on a Perkin-Elmer Model 221 spectrophotometer to determine the absorption at 2.63 μm, the absorption band of free OH^- ions in LiF.[8]

Table 2. Chemical analysis standards.

Sample No.	Amount of oxygen added (ppm)	Amount initially present (ppm)	Total oxygen (ppm)
1	1463	3.9	1467
2	407	3.9	411
3	156	3.9	160
4	14.5	3.9	18.4
5	0	3.9	3.9

The ultraviolet optical absorption coefficients of cleaved sections of each crystal grown, as well as a cleaved section of the ^7LiF from ORNL, were measured using the following equipment:

- A McPherson Model 218 0.3-m UV monochromator, equipped with a 1200-line/mm grating. The resolution of the monochromator with this grating, a 35-μm entrance slit, and a 150-μm exit slit was 0.5 nm at 121.6 nm. The monochromator was attached to an oil diffusion pump—mechanical pump system which kept the absolute pressure in the monochromator below 5×10^{-5} Torr during all the measurements.
- A McPherson Model 630 capillary discharge light source, connected directly to the entrance port of the monochromator. The gas supply for the light source was commercial hydrogen. The power supply was a McPherson Model 740 spectrographic light source power supply. Typical power levels were 2 to 3 kW. The light source was differentially pumped with a

mechanical vacuum pump through a dry-ice trichlorethylene trap, to allow the lamp to be run at useful pressures (near 1 Torr) without raising the monochromator pressure excessively.

• A McPherson, Model 651, dual-position detector housing. This housing contained space for mounting a sample holder and two positions to mount a detector in-line or 90 deg to the exit beam. Only the in-line position was used. A four-position sample holder was constructed so that one of two samples, an open port or a blank plate of stainless steel, could be rotated into the exit beam. The detector was an EMI 6256 photomultiplier type, with sodium salicylate coated on the entrance face as a wavelength shifter.

• An LLL Model LE13849 IM3, powered NIM Bin containing:

A Velonex, Nimpac Model 500-3000 V dc, 10 mA, power supply,
An LLL Model LEA72-6018, current-to-frequency converter,
A Power Designs Model AEC650 6 V dc power supply,
An LLL Model LEA67-6064 linear count-rate meter,
A Hewlett-Packard Model 5590A scaler-timer, and
A Hewlett-Packard Model 680 strip chart recorder.

Figure 4 is a block diagram of the electronics package.

• A specially constructed flange was mounted between the monochromator and the sample detector housing. This flange held a quartz window which was inserted into the beam for all measurements above 160 nm to eliminate second-order line

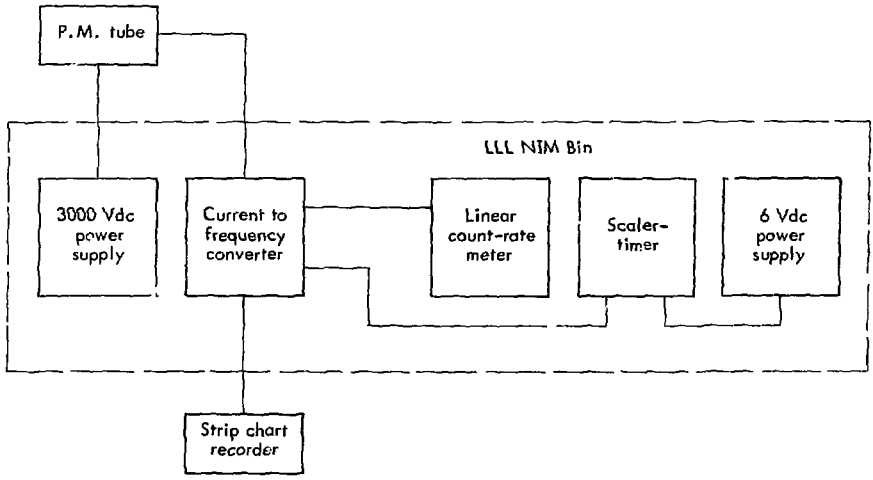

Fig. 4. Spectrophotometer detector and readout electronics.

from the spectrum. The insertion of this window at wavelengths below its fundamental absorption edge (160 nm)[32] allowed the estimation of the scattered light intensity.

The optical absorption coefficient data were taken as follows:

1. Readings were taken every 4 nm between 100 and 400 nm.

2. Readings were taken by rotating the various samples, blanks, etc., into the beam without disturbing the wavelength setting of the monochromator. Readings were integrated over 1 sec if the rate was over 1000 counts/sec, or 10 sec otherwise.

Each sample was exposed to ^{60}Co γ rays and its optical absorption coefficient was remeasured. For irradiations, the samples were nested in stainless steel wool and sealed in a Varian "Con-Flat" vacuum flange with two blank-off plates. The loading of the flange was done in the glove box under a UHP He atmosphere. The flange and plates were sealed with copper gaskets which allowed the samples to be annealed in a controlled atmosphere, if desired.

The exposure to the outside of the container was 5×10^5 or 10^6 R. The dose to the samples was not measured, but was calculated to be 3.3×10^5 or 6.6×10^5 rad, respectively, for the two exposures.

TL MEASUREMENTS

Selected portions of each crystal, or a portion of the ^7LiF starting material, were crushed with a mortar and pestle so that they were between 80 and 200 mesh. The samples were volumetrically apportioned into aluminum tubes and the ends of the tubes were crimped off. Each tube then contained ~30 mg of material, enough for two TL measurements.

The tubes were then removed from the glove box and irradiated with ^{60}Co γ rays at various doses from 700 to 10,000 rad. The samples were then allowed to sit for a few days to allow the decay of any low-temperature luminescence that may have been induced.

The TL of a sample was then read out on a specially constructed powder reader. Repeat readings were made whenever possible.

Figure 5 depicts the TLD powder reader system. To read a sample with this system, the following steps were performed:

(1) A volumetrically measured amount of sample to be read was placed on the heater; (2) a heating rate and maximum temperature were selected; and (3) the start button was pushed.

The system performed the following functions:

1. Heated the powder at the desired rate using the feedback circuitry of the temperature controller;

2. Filtered the light from the sample and heater through a Corning 4-96 bandpass filter to attenuate the I.R. contribution from the heater and any light leaks not in the filter pass band;

3. Digitized the P.M. signal through the recycling integrator;

4. Determined sampling intervals by means of the readout control;

5. Measured the integrated TL output for a single run by means of the LE8400 scaler;

6. The scaler-timer and the digital voltmeter sent time sequential information to the computer interface.

The data from a single run were stored in the computer as two vectors. One was a set of digital voltmeter (temperature) readings, the other a set of TL readings. This information could be displayed graphically on the display scope and outputted to either the DECwriter or the PC-11 punch. Since further data reduction was desired, the data were put on paper punch tape.

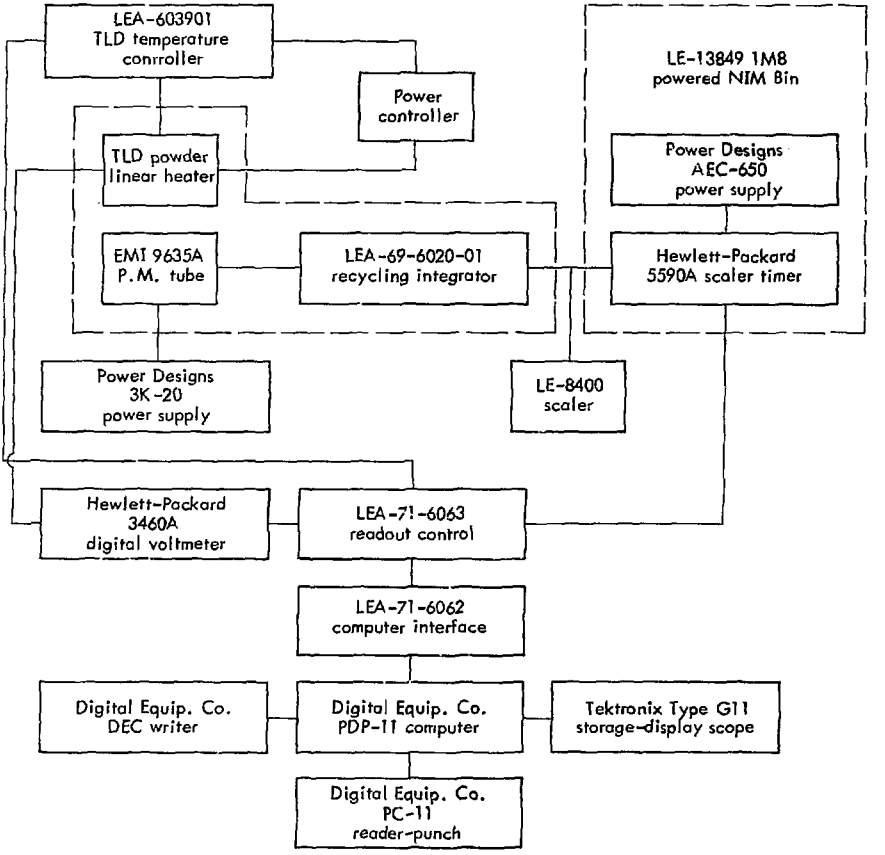

Fig. 5. TLD powder reader and computer interface.

Results

CHEMICAL ANALYSIS

The crystals were cleaved (under a UHP He atmosphere) into slabs 2-4 mm thick. The relative location of the slabs from crystal AJ-3 was not known, but for the other crystals, the position within the crystal was noted and the slabs numbered from the tip of the crystal. Figure 6 shows an idealized crystal schematically; how it cleaved, the direction of growth, and the slab numbering system.

Figure 7 is a graph of the quantity of CO_2 measured by mass spectrometer, expressed as counts/mg of sample, as a function of nominal oxygen concentration. This figure was produced as follows:

1. A weighted, linear, least-squares regression line of the form $y = bx$ was fitted to the data from samples 1 through 4, where y_i was the CO_2 counts per milligram of sample, and x_i was the concentration of oxygen added to the sample. The regression line so obtained was used to calculate the amount of oxygen initially present in sample 5, the pure ^7LiF. The amount (3.9 ppm) was used to correct the oxygen concentration of samples 1 through 4 to the total oxygen.

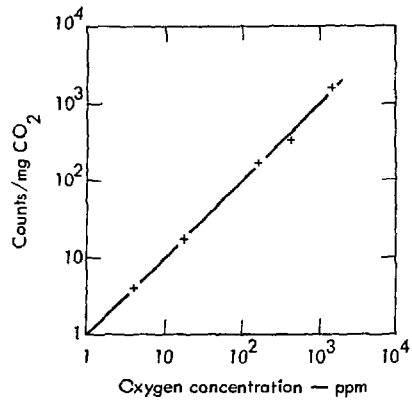

Fig. 7. Mass spectrometer output versus oxygen concentration.

2. A new least-squares regression line was calculated, using the same model as before but including sample 5. The final regression equation is

$$y\ (CO_2\ \text{counts/mg of sample}) = 1.024 \times (\text{ppm oxygen}).$$

3. The regression coefficient (1.024) changed by ~1% with the correction for oxygen initially present and the inclusion of sample 5 in the analysis. Consequently, the amount of oxygen estimated to be present initially differs by <1% for the two regression equations.

Table 3 gives the results of the chemical analysis of sections of the crystals grown for this investigation. The first sample in this table, the ORNL ^7LiF, is

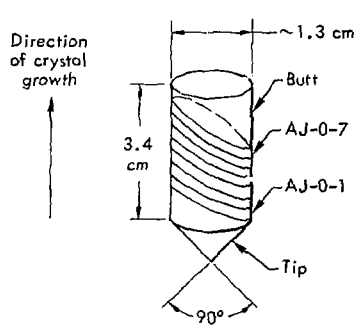

Fig. 6. An idealized ^7LiF crystal.

Table 3. Results of chemical analysis.

Sample	Measured oxygen (ppm, wt/wt)	Estimated accuracy (ppm at 1σ)
ORNL ^{7}LiF	3.90	±0.30
AJ-3	7.47	±0.57
AJ-6-Tip	25.5	±1.6
AJ-6-Butt	34.0	±2.2
AJ-5-Tip	141.4	±7.4
AJ-5-Butt	63.8	±3.7
AJ-4-Tip	304	±16
AJ-4-5	77.6	±4.1
AJ-4-Butt	1323	±67

not from a crystal grown here, but is the pure starting material and is identical with sample 5 of Table 2. The estimated accuracy of the analysis includes the estimated errors in sample weighings, standard preparation, counting errors in the mass spectrometric analysis, and in the determination of the regression coefficient. The calculation was made at the 1σ level.

OPTICAL ABSORPTION

Infrared

Figures 8 and 9 show the relative transmittance of crystal sections AJ-6-4 and AJ-4-7, respectively. Note that the ordinate in both cases is relative, not absolute, transmittance. These figures will be used to argue for the absence of significant OH^- in the crystals.

Ultraviolet

It was determined that the "stray" light in the McPherson 218 spectrometer was not negligible. Even after considerable

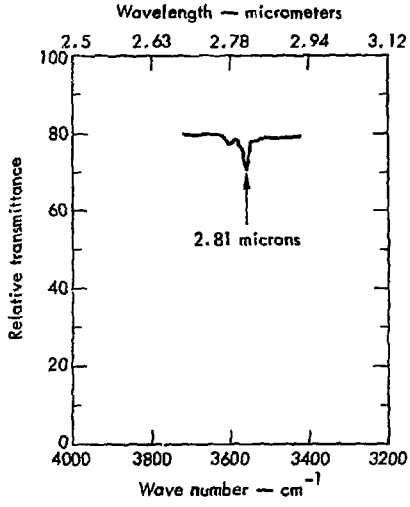

Fig. 8. Infrared transmittance of crystal section AJ-6-4.

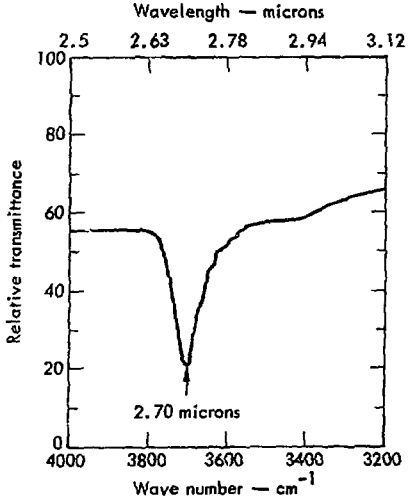

Fig. 9. Infrared transmittance of crystal section AJ-4-7.

effort to reduce its contribution, it was found that stray light constituted from a high of 50% of the light incident on the sample at wavelengths below 120 nm down to a minimum 1% of the incident light at 200 nm. Since it was determined that the amount of stray light and its transmittance in the LiF samples was not a function of the wavelength setting of the monochromator but rather depended on entrance and exit slit settings and lamp intensity, this amount of stray light incident on and transmitted by each sample was measured.

Figures 10 through 14 show the optical absorption coefficient of a section of each crystal grown, and a sample of the starting material. The absorption coefficient is determined from the equation,

$$I/I_o = (1 - R)^2 \exp(-\alpha x)$$

where I/I_o is the fraction of light of a given wavelength transmitted by the sample, corrected for stray light and background noise; x is the sample thickness; α is the optical absorption coefficient (to be calculated); and R is the coefficient of reflection determined at each wavelength by[33]

$$R = \left[\frac{n_1 - 1}{n_1 + 1}\right];$$

and n_1 is the index of refraction of LiF.

The index of refraction was calculated as a function of wavelength by fitting tabulated values of the index[34] with a ninth-degree polynomial (below 280 nm) or a straight line (280 nm to 400 nm).

The error bars on Fig. 11 indicate the precision of the optical absorption coefficient measurement at the 1σ level for wavelengths near the wavelength for which

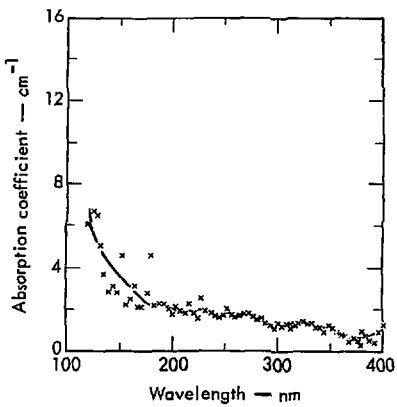

Fig. 10. Optical absorption coefficient of unirradiated ORNL ^{7}LiF.

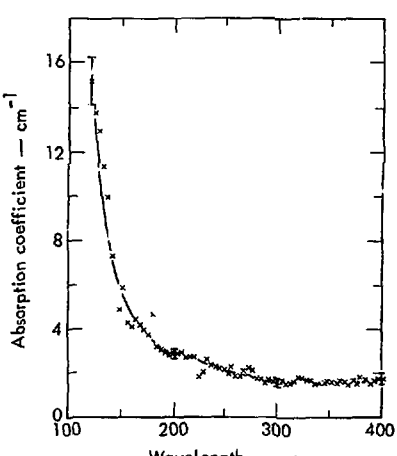

Fig. 11 Optical absorption coefficient of unirradiated AJ-3-0-2.

the error estimates were actually calculated. The error calculations include errors in the measurement of incident and transmitted light of the nominal wavelength, incident and transmitted stray light, and sample thickness. The fact that the error bars are much larger at large values of the optical absorption coefficient is a result of the relatively large stray light correction which must be applied when the transmission of the crystal is low

Figures 15 through 19 show the change in the optical absorption as a result of exposure to 5×10^5 R of ^{60}Co gamma radiation. At the 1σ level, the error bars on Fig. 16 show the precision of the measurements at wavelengths near the wavelength for which the error bar was actually calculated. The comments on the size of the error bars in Fig. 11 also apply here.

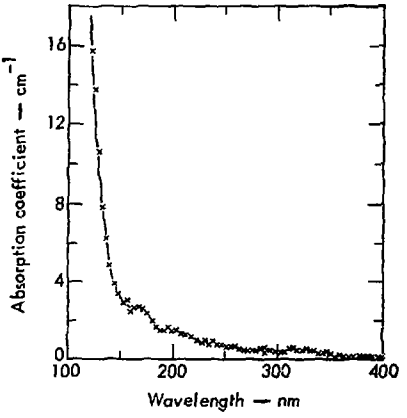

Fig. 12. Optical absorption coefficient of unirradiated AJ-6-2-1.

THERMOLUMINESCENCE

The glow curves for samples of ORNL ^7LiF crystal AJ-6 are shown in Figs. 20 and 21. The glow curves of

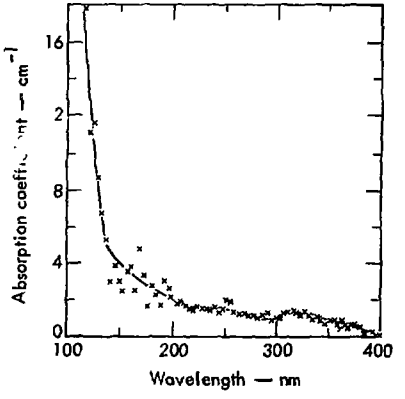

Fig. 13. Optical absorption coefficient of unirradiated AJ-5-2-1.

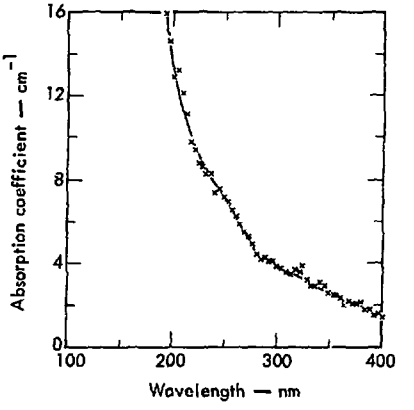

Fig. 14. Optical absorption coefficient of unirradiated AJ-4-4-1.

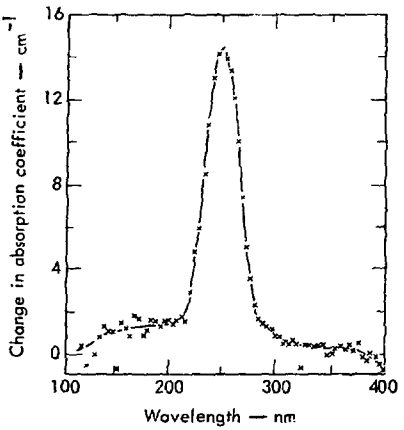

Fig. 15. Change in optical absorption coefficient after irradiation, ORNL ^{7}LiF.

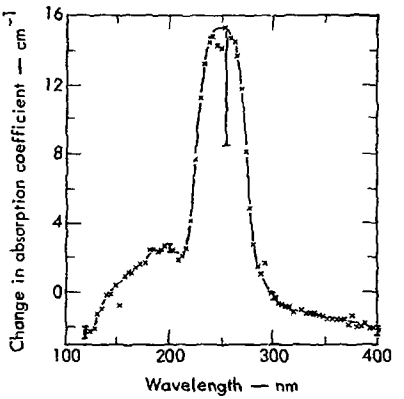

Fig. 16. Change in optical absorption coefficient after irradiation, AJ-3-0-2.

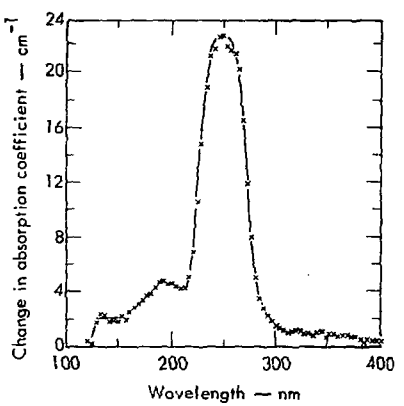

Fig. 17. Change in optical absorption coefficient after irradiation, AJ-6-2-1.

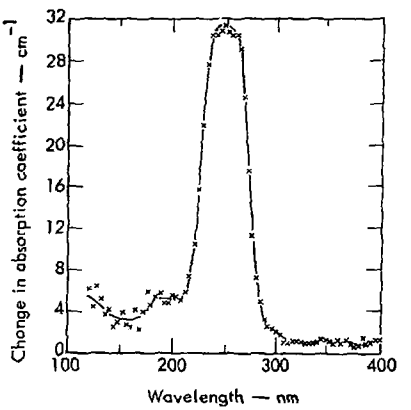

Fig. 18. Change in optical absorption coefficient after irradiation, AJ-5-2-1.

samples of ORNL ^{7}LiF at all exposures used were qualitatively like that of Fig. 20. The glow curves of all crystals grown for this investigation, at all exposures, were qualitatively similar to that of Fig. 21.

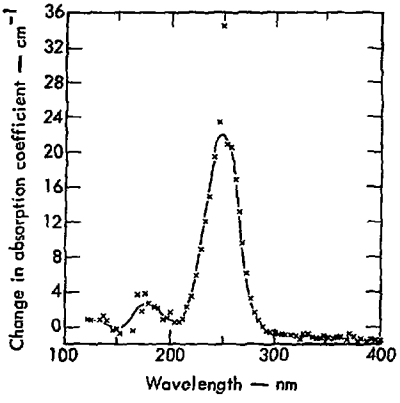

Fig. 19. Change in optical absorption coefficient after irradiation, AJ-4-4-1.

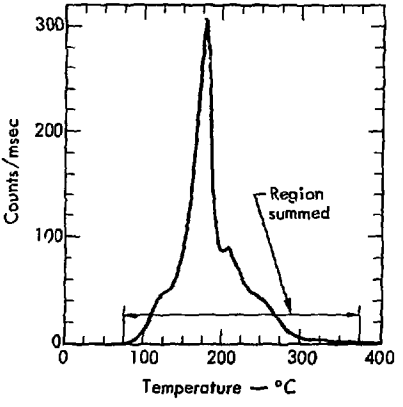

Fig. 20. Glow curve for ORNL ^{7}LiF.

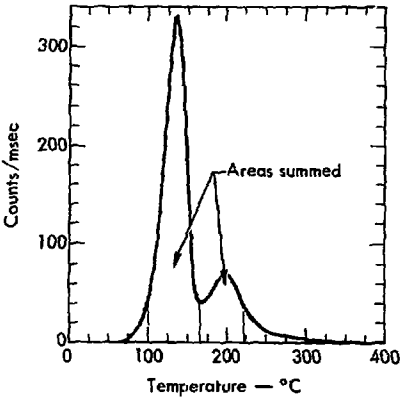

Fig. 21. Glow curve for AJ-6.

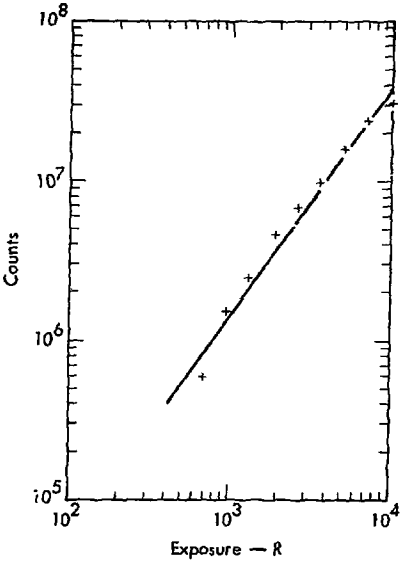

Fig. 22. Thermoluminescence of ORNL ^{7}LiF.

The counts from certain temperature regions of these glow curves were summed to produce graphs of TL response as a function of γ-ray exposure. Glow curves from the crystals grown for this investigation were summed over two regions, 99° to 169°C, and 169° to 224°C, as shown in Fig. 21. The ORNL ^{7}LiF glow curves do not exhibit the well-separated peaks of the regrown samples. Therefore, the ORNL ^{7}LiF glow curves were summed from 74° to 374°C. The net counts in these regions, for the various samples, as a function of exposure are shown in Figs. 22 through 26. The lines through the data points in the figures are least-squares regression lines calculated using the logarithm of the coordinates of each data point

Except for Fig. 22 which gives data for the ORNL ^{7}LiF material, the response of the samples to radiation is adequately described by a power function of the form

$$y = Ka^{bx}$$

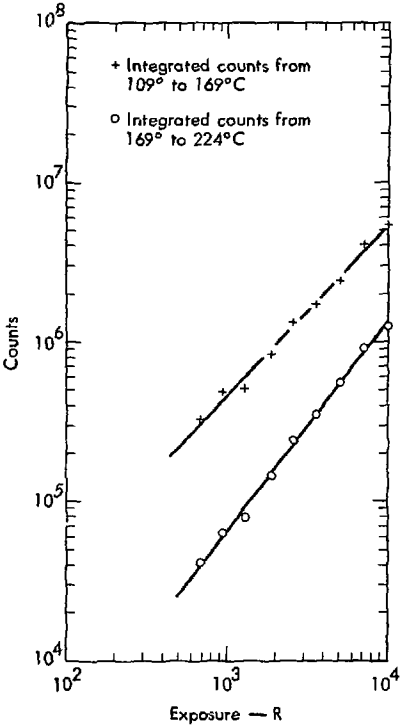

Fig. 23. Thermoluminescence of crystal AJ-3.

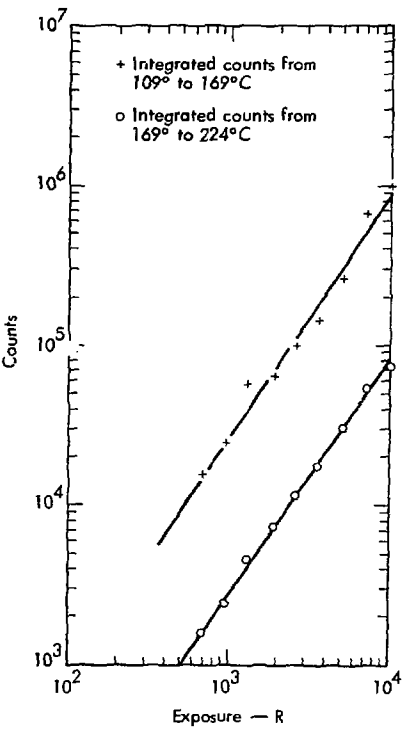

Fig. 24. Thermoluminescence of crystal AJ-4.

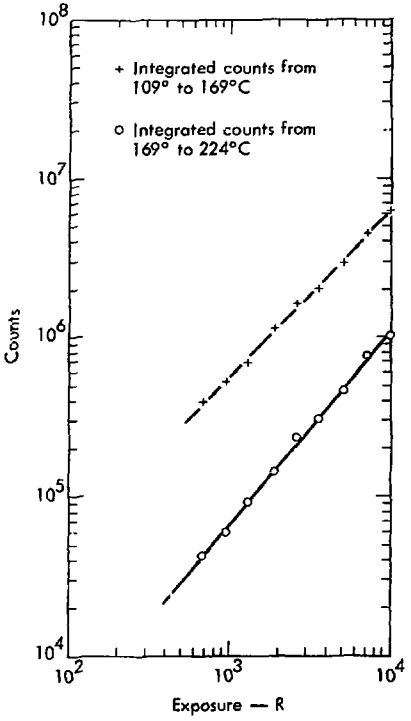

Fig. 25. Thermoluminescence of crystal AJ-5.

where the average value of b for all the regrown samples is $\bar{b} = 1.25$, and the range for b is 1.05-1.45.

Since the fit of the regression line to the data represented in Fig. 22 is significantly improved by the addition of a term in exposure squared, i.e.,

$$y = d(x)^b (x^2)^c$$

as determined by an F-test at the 99% confidence level,[35] the data were not included in the calculation of $\bar{b}$.

The data point at 687-R exposure is rejectable by Chauvenet's Criterion.[36] However, there are no experimental reasons to reject the data, and so they are included in the calculations of the regression coefficients. Because of the anomalies, no conclusions will be based on the results shown in Fig. 22.

Figure 27 shows the variation in TL sensitivity as a function of oxygen concentration for three exposure levels. The oxygen concentrations for the samples

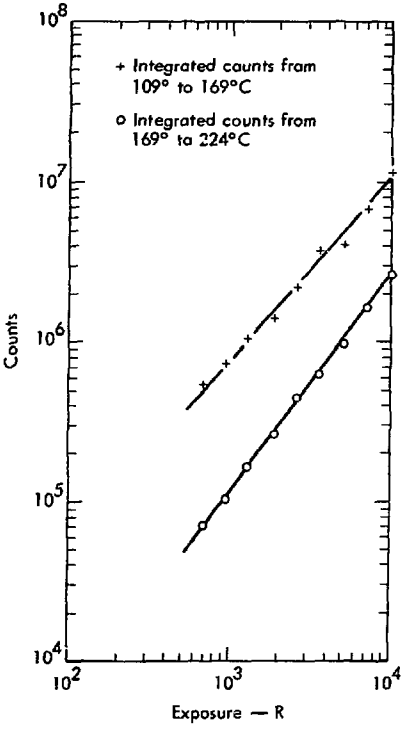

Fig. 26. Thermoluminescence of crystal AJ-6.

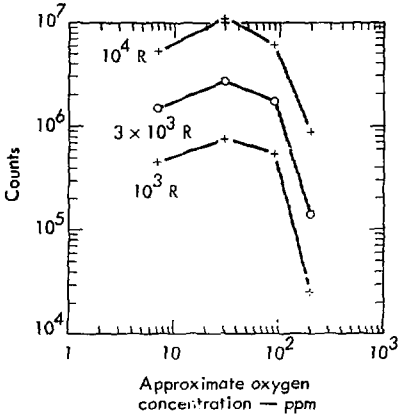

Fig. 27. TL as a function of oxygen concentration.

were assigned a linear interpolation where position within the crystal was known, or were assigned the value determined for the crystal where position was not known (sample AJ-3, 7 ppm O). This figure demonstrates the role oxygen has on TL in LiF. (See Discussion, Thermoluminescence.)

Discussion

INFRARED ABSORPTION

The absorption band associated with free OH^- ions in the LiF lattice is centered at 3730 cm^{-1} and has a width of 40 cm^{-1}.[37] Figure 9 the infrared absorption spectrum of crystal section AJ-4-7, shows an absorption band centered at 3700 cm^{-1}. This crystal section is from near the butt end of AJ-4, and is visibly cloudy. This would suggest a suspended Li_2O precipitate phase, with an estimated oxygen concentration of over 1000 ppm.

If the entire OH^- absorption band were displaced to 3700 cm^{-1} by the precipitate phase, the size of the band would indicate an OH^- concentration of approximately 100 ppm,[37] or 10% of the total oxygen content. The infrared spectrum of crystal section AJ-6-4 (Fig. 8) indicates that 10% would be the maximum fraction of oxygen that could exist as OH^- since a higher fraction would be expected to show absorption in the region of 3730 cm^{-1}.

ULTRAVIOLET ABSORPTION

It has been calculated that OH^- ions should produce an absorption band at 34 nm.[38] The lack of this absorption band in any of the crystal sections measured is taken as additional evidence that the oxygen present in these samples is not present as OH^- to any large extent.

The attempt to correlate oxygen concentration with any particular feature in the ultraviolet absorption spectrum of LiF, either irradiated or unirradiated, produced negative results (see Figs 10 to 19). In the unirradiated samples, one can see that regrowing the ^7LiF with any or no added Li_2O produces an increase in the far UV absorption (120-150 nm). Additionally, the highest concentration

sample used (AJ-4-4-1, ~200 ppm oxygen) shows increased absorption everywhere in the UV.

The single absorption band produced in all crystals by irradiating the samples is the F-band[39] which is an intrinsic defect consisting of an electron at an anion vacancy.

The loss of UV transmission in crystals AJ-4-4-1 and AJ-4-2-1 (not shown, but similar to AJ-4-4-1, Fig. 14) may indicate the appearance of a precipitate phase which upsets the crystal structure of LiF, although the sections were not visibly cloudy, as was section AJ-4-7 (see *Discussion, Infrared Absorption*). Although the ionic radius of $O^=$ would make it seem that the solubility of Li_2O in LiF should be high, Haven[25] has proposed that the energy difference between crystalline Li_2O and Li_2O in an LiF crystal limits the solubility.

Assuming that the loss of transmission is an indication of the limit of solubility, the solubility of Li_2O in LiF can be estimated at 100-200 ppm (weight fraction) since crystal section AJ-5-2-1 (concentration estimated at ~100 ppm) does not show any excess loss of UV transmission.

THERMOLUMINESCENCE

Since the glow curves from the ORNL starting material are so different from the glow curves of all the crystals grown here, no comparisons between the two will be made.

A theoretical model relating the luminescence efficiency of a substitutionally activated inorganic phosphor has been developed.[40] Assuming that the activators are randomly distributed within the crystal and that activators must be separated by some distance to be capable of luminescence, they derive an expression for luminescence efficiency. The expression is

$$\eta = \frac{c(1-c)^z}{c + (\sigma/\sigma')(1-c)}$$

where η is luminescence efficiency and c is activator mole fraction, σ/σ' and z are adjustable parameters.

σ/σ' is the nonactivator to activator capture cross-section ratio and z is related to the minimum number of possible sites surrounding an activator which may not be filled by a second activator without quenching the luminescence.

Figure 28 is a graph of relative TL response as a function of oxygen concentration. The theoretical curve was fitted to the data points at 7, 30, and 90

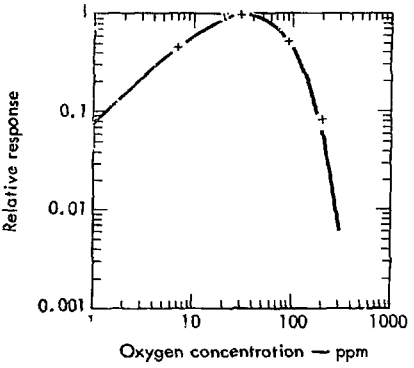

Fig. 28. Relative TL response as a function of oxygen concentration.

ppm O. The equation with the numerical values for the adjustable parameters is

$$\eta' = \frac{c(1 - c)^{24000}}{c + (3.4 \times 10^{-5})(1 - c)}$$

where η' = relative efficiency = $K\eta$.

The data point at 200 ppm O was not considered in the fitting process because the optical measurements on samples from the same crystal (AJ-4) indicated the possibility of a precipitate phase and because the assignment of oxygen concentration for this crystal was exceptionally imprecise. The agreement between theory and experiment for this point must be regarded as fortuitous.

From the above, it seems reasonable to assign the role of luminescence activator to oxygen. It does not seem reasonable to guess that oxygen functions as either a productive or competitive trapping site because the response as a function of oxygen concentration would be either monotonically increasing or decreasing, respectively, with increasing oxygen concentration.

DeWerd and Stoebe[22] have shown that OH^- acts as a competitive trap in LiF. The fact that response as a function of exposure is supralinear ($y = x^{1.25}$) over the range of exposure studied is taken as further evidence that little OH^- is present in these crystals. That is, the TL response of the TLD-100 to radiation is linear when the OH^- is competing with the TL traps for the electrons produced by radiation (for exposures <1000 R) and supralinear ($y = x^{1.2}$) after the competing traps are filled. Since the number of TL traps in pure LiF must be much smaller than the number in LiF:Mg, and since the response of the material here is supralinear at the lowest exposure levels (700 R), the possible amount of OH^- present must be limited.

CHEMICAL FORM

Although the oxygen was introduced into the lithium fluoride as Li_2O, it is possible that it exists in the lattice as some other chemical species. No work has been done here to identify the form of oxygen in the lattice, so qualitative arguments only will be advanced.

Several pieces of evidence have previously been considered which reject the possibility of OH^- as the principal species.

O_2^- has been introduced into various alkali halides and found to act as a luminescence center.[23] However, the crystals were grown in an oxygen-enriched atmosphere, and in all the crystals so grown, an absorption band near 250 nm was associated with the O_2^-. Since the crystals grown here were grown in a pure He atmosphere and no absorption band was found at 250 nm, the principal oxygen species here is probably not O_2^-.

The most likely form, then, is $O^=$ directly from the Li_2O, but other possibilities, such as O^-, are not eliminated.

CONCLUSIONS

- It is possible to grow crystals of LiF with varying oxygen content.
- The introduction of oxygen into LiF by the methods described here does

not produce a detectable oxygen absorption band in the wavelength region from 120 to 400 nm.

- The presence of oxygen in pure LiF does affect the thermoluninescence of LiF.
- The most probable role of oxygen in the thermoluminescence of LiF is as a luminescence center.

References

1. J. R. Cameron, N. Suntharalingam, and G. N. Kenney, Thermoluminescent Dosimetry (University of Wisconsin Press, Madison, Wisconsin, 1968).
2. E. E. Angino and N. Grogler, Thermoluminescence Bibliography, TID-3911, Clearinghouse for Federal Scientific and Technical Information (CFSTI), National Bureau of Standards (NBS), U.S. Department of Commerce (USDC), Springfield, Virginia, 22151 (1962).
3. F. H. Attix, Ed., Luminescence Dosimetry, CONF-650637, CFSTI, NBS, USDC (1967).
4. F. M. Lin and J. R. Cameron, "Bibliography of Thermoluminescent Dosimetry," Health Phys. 17, 349 (1969).
5. Z. Spurny, "Additional Bibliography of Thermoluminescent Dosimetry," Health Phys. 17, 349 (1969).
6. J. A. Auxier, K. Becker, and E. M. Robinson, Eds., Proceedings of the Second International Conference on Luminescence Dosimetry, CONF-680920, CFSTI, NBS, USDC, (1968).
7. F. M. Cox, "New Solid Lithium Fluoride Thermoluminescent Dosimeters," in Proceedings of the Second International Conference on Luminescence Dosimetry, pp. 60-77 (1968).
8. L. A. DeWerd and T. G. Stoebe, "Thermoluminescent Properties of Solids and Their Applications " Am. Scientist, 60, 303 (1972).
9. E. W. Claffy, "Thermoluminescence and Color Centers in Lithium Fluoride," in Luminescence Dosimetry, pp. 74-85 (1967).
10. D. W. Zimmerman, C. R. Rhyner, and J. R. Cameron, "Thermal Annealing Effects on the Thermoluminescence of Lithium Fluoride," in Luminescence Dosimetry, pp. 86-100 (1967).
11. M. R. Mayhugh, R. W. Christy, and N. M. Johnson, "Color Centers and the Thermoluminescence Process in LiF:Mg," in Proceedings of the Second International Conference on Luminescence Dosimetry, pp. 294-301 (1968).
12. E. W. Claffy, C. C. Klick, and F. H. Attix, "Thermoluminescence Processes and Color Centers in LiF:Mg," in Proceedings of the Second International Conference on Luminescence Dosimetry, pp. 302-309 (1968).
13. R. W. Christy, N. M. Johnson, and R. R. Wilbarg, "Thermoluminescence and Color Centers in LiF," J. Appl. Phys. 38, 2099 (1967).
14. C. C. Klick, E. W. Claffey, S. G. Gorbics, F. H. Attix, J. H. Schulman, and G. G. Allard, "Thermoluminescence and Color Centers in LiF:Mg," J. Appl. Phys. 38, 3867 (1967).
15. M. R. Mayhugh, R. W. Christy, and N. M. Johnson, "Thermo uminescence and Color Center Correlations in Dosimetry LiF," J. Appl. Phys. 41, 2968 (1970).

16. M. R. Mayhugh, "Color Centers and the Thermoluminescence Mechanism in LiF," J. Appl. Phys. 41, 4776 (1970).

17. M. R. Mayhugh, Color Centers and Thermoluminescence in LiF, Thesis, Dartmouth College, Hanover, New Hampshire (1970).

18. D. W. Zimmerman, D. E. Jones, and K. F. Petrock, "Photo- and Thermoluminescence of LiF: (Mg, Ti)," in Hazards Control Progress Report No. 25, Lawrence Livermore Laboratory, Rept. UCRL-50007-66-1, pp. 1-7 (1966).

19. J. Mort and D. W. Zimmerman, "Photo-Luminescence of the Z_3 Center in LiF:Mg," Phys. Letters 21, 273 (1966).

20. M. J. Rossiter, D. B. Rees-Evans, S. C. Ellis, and J. M. Griffiths, "Titanium as a Luminescence Centre in Thermoluminescent Lithium Fluoride," J. Phys. D, Appl. Phys. 4, 1245 (1971).

21. C. R. Wilson and D. E. Jones, "The Thermoluminescent Emission Spectrum of LiF," in Hazards Control Progress Report No. 32, Lawrence Livermore Laboratory, Rept. UCRL-50007-68-3, pp. 1-5 (1968).

22. L. A. DeWerd and T. G. Stoebe, "The Influence of Hydroxide Impurities on Thermoluminescence in Lithium Fluoride," in Proceedings of the Third International Conference on Luminescence Dosimetry, 1971, in press.

23. J. Rolf, F. R. Lipsett, and W. J. King, "Optical Absorption and Fluorescence of Oxygen in Alkali Halide Crystals," Phys. Rev. 123, 447 (1961).

24. R. C. Weast, Ed., Handbook of Chemistry and Physics, 46th ed. (1965).

25. Y. Haven, "The Solubility of Mg F_2 in Solid LiF," Recueil des Travaux Chimiques des Pays-Bas, 69, 1505 (1950).

26. C. F. Weaver, et al, The Production of LiF Single Crystals with Selected Isotopic Ratios of Lithium, Oak Ridge National Laboratory Rept. ORNL-3341 (1964).

27. C. A. Jacobsen, Ed., Encyclopedia of Chemical Reactions, vol IV (Reinhold Publishing Corp., New York, 1951) p. 367.

28. A. J. Singh, R. G. Ross, and R. E. Thoma, Zone Melting of Inorganic Fluorides, Oak Ridge National Laboratory Rept. ORNL-3658 (1964).

29. A. J. Singh, R. G. Ross, and R. E. Thoma, "Vacuum Distillation of LiF," J. Appl. Phys. 36, 1367 (1965).

30. Research Organic/Inorganic Chemical Corp., Inorganic Chemicals Catalog, p. 71 (1972).

31. E. Walter, private communication (1972).

32. J. A. R. Samson, Techniques of Vacuum Ultraviolet Spectroscopy (J. Wiley and Sons, New York, 1967) p. 181.

33. D. R. Corson and P. Lorrain, Introduction to Electromagnetic Fields and Waves (W. H. Freeman and Co., San Francisco, 1962) p. 371.

34. D. M. Roessler and W. C. Walker, "Optical Constants of Magnesium Oxide and Lithium Fluoride in the Far Ultraviolet," J. Opt. Soc. Am. 57, 835 (1967).

35. N. R. Draper and H. Smith, Applied Regression Analysis (John Wiley and Sons, New York, 1966) pp. 71,72.

36. G. D. Chase and J. L. Rabinowitz, Principles of Radioisotope Methodology (Burgess Publishing Co., Minneapolis, Minn., 1968) pp. 104-107.

37. T. G. Stoebe, "Influence of OH^- Ions on Infrared Absorption and Ionic Conductivity in Lithium Fluoride Crystals," J. Phys. Chem. Solids 28, 1375 (1967).

38. M. J. Rossiter, D. B. Rees-Evans, and S. C. Ellis, "Preparation of Thermoluminescent Lithium Fluoride," J. Phys. D, Appl. Phys. 3, 1816 (1970).

39. J. V. R. Kaufman and C. D. Clark, "Identification of Color Centers in Lithium Fluoride," J. Chem. Phys. 38, 1388 (1963).

40. P. D. Johnson and F. E. Williams, "The Interpretation of the Dependence of Luminescent Efficiency on Activator Concentration," J. Chem. Phys. 18, 1477 (1950).